Comparison of safety levels required by adequate regulations for cargo ships of different types

Piotr Szulczewski

https://orcid.org/0000-0001-7293-0854

Gdańsk University of Technology
Florida Institute of Technology
e-mail: p_szulczewski@yahoo.com

Abstract
During the currently ongoing development of methods for assessing the safety of ships, it is imperative that a compromise between the accuracy of the results and the accessibility of obtaining results is reached. This paper shows the calculations of a theoretical hull against damage stability regulations as included in SOLAS 2020, ICLL 66/88 as amended in 2003 and MARPOL 78. The rules included in the currently valid regulations require certain righting arm curve properties from vessels before and after potential damage, which does not pose a high difficulty level to engineers. However, for many engineers and scientists working with these rules, it is unclear what kind of behavior (particularly roll motion) these righting arm curve parameters correspond. In this paper, a correlation between the required GZ properties and the actual roll motion of a ship in waves, as calculated with the well-established method proposed by the ITTC, is revealed, and a comparison of the results to the currently in use regulations as well as comparison between the methods themselves is made. The comparison reveals the impact of GZ curve parameters on the roll motion of the ship.

Introduction

The current structure of rules governing the safety of ships is very complex. This is mainly because of a complex relationship between the Flag States, Classification Societies, and the Owners/Operators of the ships. To simplify this relationship in broad terms, it is possible to state that it is the Flag State of the country a ship is flying that guarantees fulfilling all the mandatory safety requirements. Therefore, it is in the Flag's hands to determine if a ship is seaworthy and adequately equipped. Needless to say, many Flag States do not have the resources to monitor all the criteria responsible for checking if a sufficient range of positive righting lever curve is provided. For cargo ships, for which the SOLAS 2020 method is used, the rules defined by ICLL 66 as amended or

SOLAS 90 were previously applicable (except for special purpose ships).

The IACS (International Association of Classification Societies) merchant fleet constitutes approximately 96% of the worldwide fleet (tonnage-wise) and 75% of worldwide fleet (unit number-wise). The remaining fleet may be governed by some Flag States directly or other small Classification Societies which are not members of the IACS. It is important to note that, in many cases, the ships that are not classed by an IACS Classification Society do not meet IACS minimum requirements.

It is not easy to list all the requirements related to safety from the Classification Societies (members of IACS), but the underlining factor is that they are grouped into certain categories and dealt with by different departments and people within these

organizations. This may lead to a lack of correlation between specific requirements and overseeing certain safety aspects resulting from ships combined characteristics. The main disadvantage of the rules/requirements is their selective structure which introduces a high risk of being in contrast with the holistic approach to safety. In this work, a direct seakeeping calculation of a selected example vessel is presented, and the results are compared with the rules, namely MARPOL 78, ICLL 66/88, and SOLAS 2020.

Due to the commercial sensitivity of the regulations, there is limited publically available literature covering the subject of determination of the safety of cargo ships and the dynamic stability investigations in damaged conditions (Gourlay & Lilienthal, 2002 – intact). Hence, this paper presents the actual levels of safety correlated to the roll motion as stipulated by the hydrostatic parameters of ships in the published regulations ICLL 66/88, MARPOL 78, and SOLAS 2020. The differences (if any) provided by these regulations safety levels will be identified.

The purpose of this work is to popularize the knowledge and understanding of the actual levels of safety provided by the currently in use rules and regulations and indicate the direction in which they should be developed.

Investigated vessel

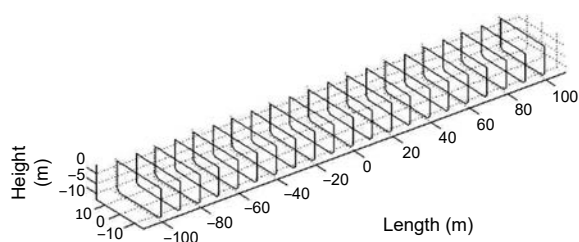The vessel (Figure 1) conditions selected for the investigation are parameters shown in Table 1.

Figure 1. Sections of the investigated vessel (Bole & Lee, 2006; Tunaley, 2013)

Table 1. Parameters of the investigated theoretical hull

Parameter	SOLAS criteria	ICLL/MARPOL criteria
Length, L	200 m	200 m
Beam, B	30 m	30 m
Draft, T	13.13 m	11.85 m
GZ_{max}	0.12 m	0.10 m
GM	0.74 m	0.22 m
Range	16 deg	20 deg
Cb	0.99	0.99

In both cases, the maximum value of the righting arm and the range of the positive value of righting arm correspond to the minimum requirements stipulated by the corresponding regulations.

Survival conditions as described in SOLAS 2020, ICLL 66/88, and MARPOL 78

As per the formula for the Attained Subdivision Index (SOLAS, 2020), the obtained for each damage case scenario "p_i" index is multiplied by the "s" factor. This factor varies with the attained stability parameters of ships for particular damage cases as defined by the factor "p_i".

In general, the "s_i" is defined as the minimum of the values presented (1):

$$s_i = \text{minimum}\{s_{\text{intermediate, }i}, s_{\text{final, }i}, s_{\text{mom, }i}\} \qquad (1)$$

However, for cargo ships, only the "$s_{\text{final, }i}$" is taken into consideration. The formula for "$s_{\text{final, }i}$" (2) is a function of stability parameters of vessels at the final stage of flooding.

$$s_{\text{final, }i} = K \cdot \left(\frac{GZ_{\text{max}}}{0.12} \cdot \frac{\text{Range}}{16} \right)^{\frac{1}{4}} \qquad (2)$$

where:
K – coefficient as per SOLAS 2020,
s – probability of a vessel surviving damage as per SOLAS 2020,
GZ – righting arm of a ship in meters,
Range – positive range of a righting arm in degrees.

In both above cases, if the values of either GZ_{max} or "Range" are larger than the denominatives, the values for calculations are not to be taken greater than them.

Consequently, there is no additional benefit for the value of the "s" factor from the values of the previously mentioned stability parameters being greater than the values stipulated in the above equations. The "K" factor in the equation for "s" is a function that determines the maximum allowable final degree of heel after sustaining damage and is only to be taken as "1" if it is less than 25 degrees and 0 if it is more than 30 degrees. In other cases, it is to be taken as a function of the difference between the maximum allowable angle of the heel and the actual angle.

A comparison table of the required stability parameters by these three methods is presented below (Table 2).

Figure 2 shows a graphical representation of values of the "s" factor for different initial parameters.

Table 2. Comparison of the survival stability criteria as per SOLAS 2020 and ICLL 66/88/MARPOL 78

| "s" factor as defined in SOLAS 2020	ICLL 66 as amended/MARPOL 78 requirements
$$s_{\text{final},i} = K \cdot \left(\frac{GZ_{\max}}{0.12} \cdot \frac{\text{Range}}{16} \right)^{\frac{1}{4}}$$	1) Final angle of heel to be less than 15 or at maximum 17 degrees. 2) The range of positive stability righting lever curve to be at least 20 degrees. 3) The minimum value of righting arm within the range as described in point 2 above to be 0.1 m (the metacentric height in the final floating condition is positive). 4) The area under the righting lever curve within the range as described in point 2 to be not less than 0.0175 m·rad.
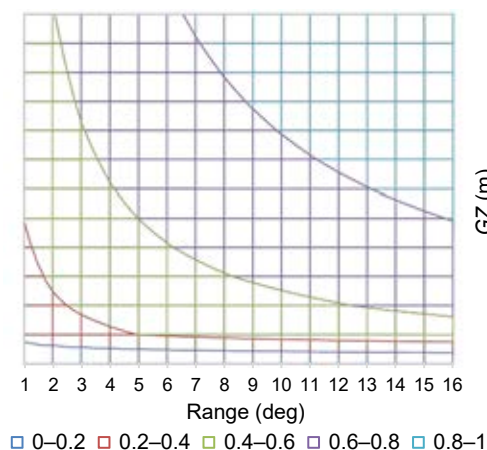
Figure 2. The value of attained s-factor for various stability parameters from SOLAS 2009

In addition, it is worth mentioning that a result of such a low value of righting arm as 0.1 meters from theoretical calculations is relatively improbable, and there may be very little practical difference between the 0.1 meters and 0.12 meters limit.

The final value of "*A*", the attained level of safety factor that is to be taken for comparison against the required safety level represented by "*R*", is taken as a sum (3) of the mean "*A*" value obtained from calculations from damage cases to both sides for different drafts: the subdivision draft (usually corresponding to the deepest subdivision draft), the partial draft, being calculated as per an adequate formula (SOLAS, 2020), and the light service draft (usually corresponding to the lightest draft that the vessel may operate in, e.g. Light ballast draft).

$$A = 0.4 A_s + 0.4 A_p + 0.2 A_l \qquad (3)$$

For cargo ships, in no case is the attained safety level calculated at any of the above mentioned drafts to be less than 0.5 multiplied by the required level of safety.

Calculation model and assumptions (methodology)

To accurately evaluate the regulations, a sea-keeping model (strip theory) of a ship on waves has been prepared. The model has the following set of assumptions:

1) The pressure under the wave-crest is modelled with the use of hydrostatics.
2) The evaluated objects have a large *L* to *B* and *L* to *H* ratios (more than 4) and are symmetric.
3) Motion amplitude is small so that equations can be linearized (Journée & Massie, 2001). This means that damping coefficients and added mass coefficients are constant in time/frequency and that motions of a ship can be calculated separately with minimum error to the results introduced (quasi-dynamical approach). (This assumption will cause an error in calculations, but as evaluated in multiple studies (e.g. Salvesen, Tuck & Faltinsen, 1970), the final values are not very far off the actual values and can be considered a good approximation).
4) The motions that have a decisive impact on a ship's survivability in waves are the motions that impact the vertical position of weather-tight openings or deck lowest point in the weather conditions. They are roll, sway, pitch, and heave. Consequently, the stability of a ship can be accurately described by the determination of the damping and added mass coefficients for the following motions: roll, sway, sway coupled with roll, heave, and pitch only.
5) The waves are non-directional and of single periodicity. (This is not the case at sea; however, the directional nature of waves was neglected to find parameters of submerged parts of the hull, the directional nature of waves was neglected).

Coordinate system

The right-handed system of coordinates (Figure 3) (Faltinsen, 1990) is fixed with the ship's center of gravity and its origin set at a waterline level. Axis *Z* goes through the center of gravity. Though selecting this model introduces some complexity to the mathematical model, it allows for a good presentation of results.
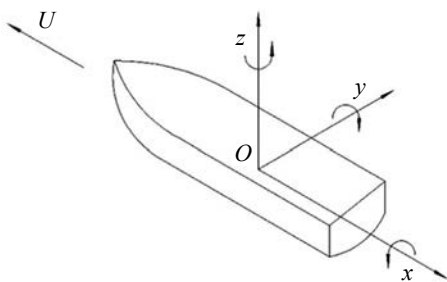
Figure 3. Selected coordinate system

Dynamic components in motion equation

The general equation governing a 6 degree of freedom ship motion can be presented as below, and further simplified and divided into the static and dynamic components (4) (Schmitke, 1978; Traintafyllou, Bodson & Athans, 1983; Faltinsen, 1990; Larsen, 2013; Szulczewski, 2017).

$$\sum_{k=1}^{6}\left[\left(M_{jk}+A_{jk}\right)\ddot{\eta}_k + B_{jk}\dot{\eta}_k + C_{jk}\eta_k\right]=$$

$$= F_j e^{i\omega t} + F_E \xrightarrow{\text{ simplified to }}$$

$$\left\{\begin{bmatrix} M & 0 \\ 0 & I_y \end{bmatrix} + \begin{bmatrix} A_{33} & A_{35} \\ A_{53} & A_{55} \end{bmatrix}\right\}\ddot{\eta}_u + \begin{bmatrix} B_{33} & B_{35} \\ B_{53} & B_{55} \end{bmatrix}\dot{\eta}_u +$$

$$+ \begin{bmatrix} C_{33} & C_{35} \\ C_{53} & C_{55} \end{bmatrix}\eta_u = \begin{bmatrix} F_3 \\ F_5 \end{bmatrix} e^{i\omega t}$$

and

$$\left\{\begin{bmatrix} M & 0 & -Mz_c \\ 0 & I_x & -I_{xz} \\ -Mz_c & -I_{xz} & I_z \end{bmatrix} + \begin{bmatrix} A_{22} & A_{24} & A_{26} \\ A_{42} & A_{44} & A_{46} \\ A_{62} & A_{64} & A_{66} \end{bmatrix}\right\}\ddot{\eta}_v +$$

$$+ \begin{bmatrix} B_{22} & B_{24} & B_{26} \\ B_{42} & B_{44} & B_{46} \\ B_{62} & B_{64} & B_{66} \end{bmatrix}\dot{\eta}_v + \begin{bmatrix} C_{22} & C_{24} & C_{26} \\ C_{42} & C_{44} & C_{46} \\ C_{62} & C_{64} & C_{66} \end{bmatrix}\eta_v =$$

$$= \begin{bmatrix} F_2 \\ F_4 \\ F_6 \end{bmatrix} e^{i\omega t} + \begin{bmatrix} F_E \\ M_E/Z \\ M_E/X \end{bmatrix} e^{i\omega t} \qquad (4)$$

where:
A_{xx} – total added mass coefficient,
B_{xx} – total roll damping coefficient,
C_{xx} – stiffness matrix,
F_k – force component, where $k = 1, 2, ..., 6$, or "s",
$\eta_{v,u}$ – position of a ship (displacement or rotation),
$I_{(y)}$ – total moment of inertia around the axis,
M_E – wave exciting moment.

The dynamic components are represented by M_{jk}, A_{jk} and B_{jk} (Bowdich, 1995; Hem Lata & Thiagarajan, 2007; Fujiwara et al., 2009; Kawahara,

Maekawa & Ikeda, 2012; Hardin, 2013; Salehi, Ghadimi & Rostami, 2014).

Derivation of dynamic components is a difficult task, and numerous attempts have been made to increase the accuracy of the obtained coefficients.

Still, the common practice remains to validate analytical/numerical simulations with tests in the ship model basin. For this method, a derivation technique has been utilized with great focus on eliminating the risk of overestimating these coefficients and limiting the complication of the calculations.

Coefficients M_{jk}, A_{jk} and B_{jk} from equation (1) depend on time and the vessel's position in relation to the sea surface. M_{jk} is called the generalized mass matrix of a ship. The M value is the mass of the ship and remains constant when afloat. Mz_c components (see (4)) are related to mass acting on the acceleration in a motion in a given coordinate system. Given the selected coordinate system at the waterline, the value of z_c is the value of the vertical position of the center of ship mass against the origin of the coordinate system. I_y, I_x, I_z, and I_{xz} are the moment of inertia values around the respective axis.

A_{jk} is called added mass coefficients matrix and directly reflects the dynamic force acting on the structure that is caused by the pressure field of the fluid being forced to oscillate by the moving structure. The added mass in the four motions taken into account is governed by the shape of the submerged body, frequency of motion, and, naturally, the size of the submerged body. It is not an easy task to accurately predict the values of added mass coefficients. However alternative methods, such as the close-fit Frank method, which were proven to offer good accuracy (Schmitke, 1978; Journée, 2001; Das, Sahoo & Das, 2006; Hem Lata & Thiagarajan, 2007; Wang et al., 2012), may be used. For example, for the derivation of necessary coefficients, a hydrodynamic model may be applied to various ranges of "mid-ship sections", and the mass parameters then transferred into a three-dimensional model using strip theory.

The roll movement is sensitive to the forces that cause it, and hence, to model it accurately, it was divided into components presented in equation (5) (ITTC, 2011) and further discretized with the use of the Kawahara method (Kawahara, Maekawa & Ikeda, 2012).

$$B_{44} = B_{44W} + B_{44L} + B_{44F} + B_{44E} + B_{44PP} (+B_x) \quad (5)$$

B_{44W} is a coefficient described as the wave making coefficient. The wave component for a two-dimensional cross-section is calculated by potential

flow theory. A calculation of the damping coefficient in sway motion for a given hull form is needed. Since analytical formulas can quite accurately and relatively easily approximate a ship's longitudinal section, calculation of the wave making component at zero speed may be performed by multiplication of this coefficient times the roll lever (6) (ITTC, 2011).

$$B'_{44W0} = B'_{22} \cdot \left(l_w - \overline{OG} \right)^2 \qquad (6)$$

The ITTC (International Towing Tank Conference) also provides a recalculation method for the wave making component at different speeds. It is important to underline that this damping component for big ocean-going cargo ships is relatively small compared to other components.

B_{44L} is a lift making component that must be added to ships moving forward and with a sway motion. It is described mainly by speed, size of the vessel, and the position of center of gravity of the ship (7) (ITTC, 2011).

$$B_{44L} = \frac{\rho}{2} VLdk_N l_0 l_R \left(1 - 1.4 \frac{\overline{OG}}{l_R} + \frac{0.7\overline{OG}}{l_0 l_R} \right) \quad (7)$$

where: $l_0 = 0.3d$, $l_d = 0.5d$.

B_{44F} is a frictional component and at zero speed can be derived from the well-known Kato's formula. Kato's formula describes this coefficient as (among others) a function of area, viscosity, and surface friction. ITTC proposes another calculation formula for ships moving at constant speed forward (8) (ITTC, 2011).

$$B'_{44F0} = \frac{4}{3\pi} \rho S_f r_f^3 \varphi_a \omega_E C_f \qquad (8)$$

B_{44E} is an eddy making component (9) (ITTC, 2011) and comes from the sectional vortices. Its relation to the hull shape was described by half breadth to draught ratio and area coefficients. These were used in this paper and are considered the industry standard. This coefficient is further recalculated if the vessel is moving at a given speed.

$$B'_{44E0} = \frac{4\rho d^4 \omega_E \varphi_a}{3\pi} C_R \qquad (9)$$

B_{44APP} is additional resistance coming from appendages such as bilge keels and rudders. All external hull appendages have some impact on the behavior of a ship. In the method proposed in this paper for the identification of physical parameters that have a decisive impact on roll motion, only the bilge keels are considered. The reason for selecting the bilge keels is that their area is usually the greatest

and that they are specifically designed to reduce ships roll movement. Their impact must be therefore taken into account. The methodology for calculating the effect from bilge keels is taken directly from the recommended components by ITTC guidelines. The B_{44APP} coefficient (concerning bilge keels) can be divided into four components (10) (ITTC, 2011).

$$B_{44APP(BK)} = B_{44KN0} + B_{44BKH0} + B_{44BKL} + B_{44BKW} \qquad (10)$$

In addition to the damping coefficients, the added mass in roll motion (A_{44}) may be approximated by a function of investigated section area, draught, and distance between the center of buoyancy and gravity of moving hull (11) (Salvesen, Tuck & Faltinsen, 1970; Faltinsen, 1990).

$$A_{44} = \rho A \left(\frac{d^3}{12} + d\overline{BG}^2 \right) \qquad (11)$$

Excitation forces

It was found that the change of the initial condition of the vessel after, e.g. tank flooding, may be represented by an excitation force added on the right side of the equation (12) (Miller, Slager & Webster, 1974; Fan & Xia, 2002; Gourlay & Lilienthal, 2002).

$$F_S = \left(-M_x - A_x \right) \ddot{\phi} - B_x \dot{\phi} - C_x \phi \qquad (12)$$

where:

$$\phi = Ae^{i\omega t}$$
$$\dot{\phi} = i\omega Ae^{i\omega t}$$
$$\ddot{\phi} = -A\omega^2 e^{i\omega t}$$
$$F_S = A_F e^{i(\omega t + \varphi)}$$

$$-\left(M_x + A_x \right) = \mathrm{Re}\left(\frac{A_F e^{i(\omega t + \varphi)} - C_x Ae^{i\omega t}}{\omega^2 Ae^{i\omega t}} \right) =$$

$$= \mathrm{Re}\left(\frac{A_F e^{i\varphi} - C_x A}{\omega^2 A} \right) = \frac{A_F \cos(\varphi)}{\omega^2 A} - \frac{C_x}{\omega^2}$$

$$B_x = \mathrm{Im}\left(\frac{A_F e^{i(\omega t + \varphi)} - C_x Ae^{i\omega t}}{\omega Ae^{i\omega t}} \right) =$$

$$= \mathrm{Im}\left(\frac{A_F e^{i\varphi} - C_x A}{\omega A} \right) = \frac{A_F \sin(\varphi)}{\omega A} - \frac{C_x}{\omega}$$

where:
A_F – force amplitude,
A – wave amplitude,
ω – wave frequency,

t – time,
φ – phase angle (lag),
$C_x = I^x \cdot \rho^x \cdot g$

The other excitation forces modelled are the forces from waves. The well-known and common practice is to measure the significant wave height. The significant wave height ($H_{1/3}$) is by definition the mean wave height (trough to crest) of the highest third of the waves and is measured by an experienced crew onboard with the naked eye. The crew onboard may relatively easily observe the height of waves, but not their period. When evaluating ocean waves' statistics to determine the risks for ocean-going ships in the shape of a harmonized method, the range of periods of waves must be evaluated.

To achieve this, the statistical correlation between significant wave heights and the wave periods was brought into a two-dimensional shape (Figure 4).
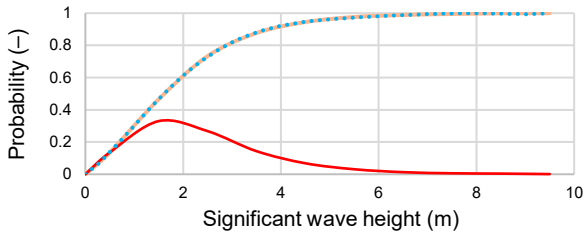

Figure 4. Example probability density function of the significant wave height based on statistical data for worldwide trade

The probability values of wave height may have a very different impact on the safety of ships depending on the shape of waves and their period. Therefore, selecting just one most probable wave period is considered a very inaccurate approximation. For this paper, the most probable wave period with waves of significant height up to 2 meters (a probability of which is estimated at more than 0.5) was investigated.

The forces from waves in the frequency domain calculation model were divided into Froude-Kriloff forces and moments and diffraction forces, and in strip theory, may be presented as integrals for each investigated strip (13), (14).

$$
\begin{bmatrix} F_2 \\ F_4 \\ F_6 \end{bmatrix} = \begin{bmatrix} \int (f_{2FK}(x) + f_{2D}(x))\,dx \\ \int (f_{4FK}(x) + f_{4D}(x))\,dx \\ \int (x(f_{2FK}(x) + f_{2D}(x)) - Ua_{22}(x_{\text{mean}})v)\,dx \end{bmatrix} +
$$

$$
+ \begin{bmatrix} U \cdot a_{22}(x_{\text{mean}})w \\ U \cdot a_{42}(x_{\text{mean}})v \\ U \cdot a_{22}(x_{\text{mean}})v \end{bmatrix} \tag{13}
$$

$$
\begin{bmatrix} F_3 \\ F_5 \end{bmatrix} = \begin{bmatrix} \int (f_{3FK}(x) + f_{3D}(x))\,dx \\ \int (x(f_{3FK}(x) + f_{3D}(x)) - Ua_{33}(x_{\text{mean}})w)\,dx \end{bmatrix} +
$$

$$
- \begin{bmatrix} -U \cdot a_{33}(x_{\text{mean}})w \\ U \cdot x_{\text{mean}} \cdot a_{33}(x_{\text{mean}})w \end{bmatrix} \tag{14}
$$

where:

$$
f_{2FK}(x) = i\rho g\zeta_a \int n_3 e^{-ik(x\cos\beta + y\sin\beta)} e^{kz}\,dl
$$

$$
f_{3FK}(x) = i\rho g\zeta_a \int n_2 e^{-ik(x\cos\beta + y\sin\beta)} e^{kz}\,dl
$$

$$
f_{4FK}(x) = i\rho g\zeta_a \int n_4 e^{-ik(x\cos\beta + y\sin\beta)} e^{kz}\,dl
$$
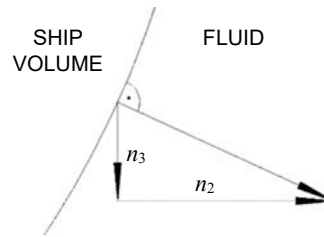
$n_4 = y\,n_2 - z\,n_3$

$f_{2D} = a_{22}(x)\,a_y + b_{22}(x)\,v$

$f_{3D} = a_{33}(x)\,a_z + b_{33}(x)\,w$

$f_{4D} = a_{42}(x)\,a_y + b_{42}(x)\,v$

a_y, a_z, v, w – initial accelerations and speeds approximated per Salvesen (Salvesen, Tuck & Faltinsen, 1970).

The accuracy of the model used (13), (14) depends on (among others) the panelization of the cross sections. If the panelization is accurate enough, the vertical and horizontal components of vector 'n' will be accurate. If, however, the panelization is not accurate or does not follow the geometry that may change rapidly at, e.g. knuckles, the error may be large and difficult to control.

Comparison of the probability of survival

There is no proven correlation between the weather conditions and the probability of hazard occurrence. Hence, for this method, long term weather statistics for the global sea waters were used as they are a good representation of the probability of encounter during an emergency. Because of the above, the statistics used for fatigue calculations may be considered valid (Figure 5) (Cummins, 1962).

For these calculations, two initial conditions from the identical geometry have been selected:
• "SOLAS" Condition: in which the maximum attained GZ is equal to 0.12 m, and the range of the positive righting arm curve is 16 degrees, as required by the rules (Figure 6).
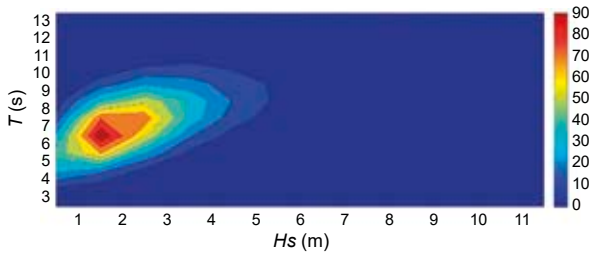
Figure 5. Frequency distribution of sea states in the function of wave periods and significant wave height for worldwide trade (total number normalized to 1000)
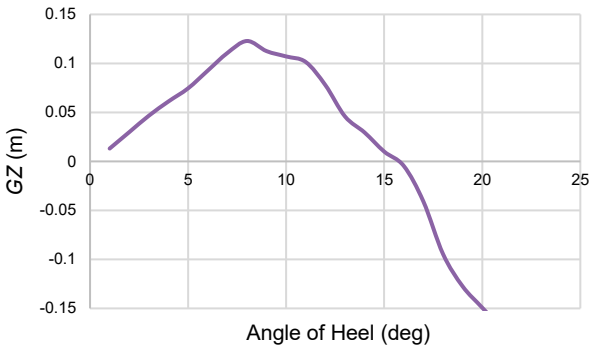

Figure 6. *GZ* righting arm curve fulfilling the SOLAS 2020 criteria (area under the *GZ* curve = 0.01801 m·rad)
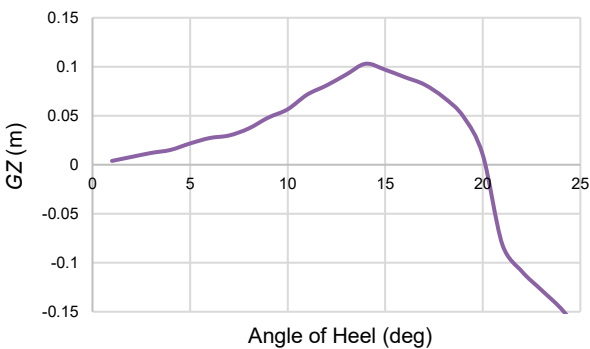

Figure 7. *GZ* righting arm curve fulfilling the ICLL 66/88 and MARPOL 78 criteria (area under the *GZ* curve = 0.01754 m·rad)

- "ICLL/MARPOL" Condition: in which the maximum attained GZ is equal to 0.10 m, and the range of the positive righting arm curve is 20 degrees, as required by the rules (Figure 7).

To obtain what may seem like a minor change of the stability righting arm curve parameters, a quite significant change in the vessel condition had to be made. The initial vertical position of the center of gravity in the ICLL condition had to be increased by 1.89 meters, and the freeboard had to be increased by 1.28 meters. This suggests that a different loading condition design may be required to fulfil these different criteria.

The resulting Righting Arm curves are presented in Figure 6, and a comparison of results is presented in Table 3.

Table 3. Comparison of roll angles in waves of vessel marginally meeting SOLAS 2020 and ICLL Criteria 66/88

	SOLAS	ICLL	Difference [%]
Hs0.5 T6	0.98	1.38	**40.8**
Hs1 T6	1.88	2.72	**44.7**
Hs2 T6	3.72	5.63	**51.3**

After analyzing dynamic behavior (Figure 8), the following roll angles in different sea states have been obtained.
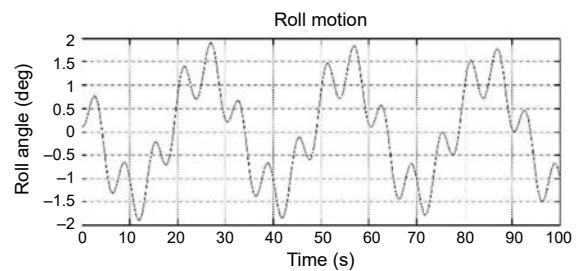

Figure 8. Sample result of rolling angle calculated over the period (here for SOLAS condition, wave height 1 m, wave period 6 s, wave direction: beam wave)

Way forward

After identifying significant differences in roll motion in waves from the vessel meeting ICLL and SOLAS 2020 criteria, an investigation of the impact of an increase of *GZ* by just 1 cm on the roll motion has been made. (The increase of maximum *GZ* by 1 cm was attained by merely lowering the center of gravity by 5 cm (Figure 9), the results from a seakeeping model are presented in Figure 10, and a comparison of results is shown in Table 4).
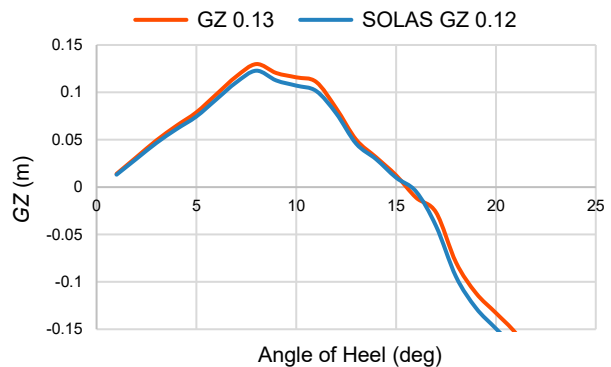

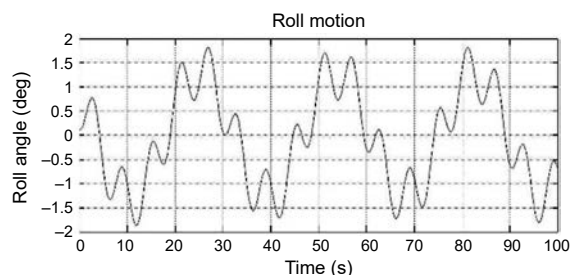**Figure 9. *GZ* righting arm curve *GZ*max = 0.13, range 16 degrees**

Figure 10. Sample result of rolling angle calculated over the 100 s period (for the loading condition in question, wave height 1 m, wave period 6 s, wave direction: beam wave)

Table 4. Comparison of roll angles in waves of vessel meeting SOLAS 2020 and with GZ_{max} increased by 1 cm

	GZmax = 0.12	GZmax = 0.13	Difference [%]
Hs0.5 T6	0.98	0.94	**–4.1**
Hs1 T6	1.88	1.8	**–4.3**
Hs2 T6	3.72	3.57	**–4.0**

The seakeeping model used to evaluate the seakeeping in this work may be considered an industry standard. However, theoretical seakeeping calculations must be validated with model tests or other industry recognized methods/software.

Conclusions

This paper's results clearly identify that a vessel fulfilling the SOLAS criteria can be significantly less prone to large amplitudes of roll motion and hence possible flooding of deck and openings on deck (by over 40% in the investigated sea states). In other words, the shape of the righting arm as required by SOLAS 2020 regulations guarantees a significantly better response to wave excitation forces, increasing the chance of a vessel remaining in a safe condition after damage.

The requirement as stipulated by SOLAS 2020 provides stability conditions in which vessels are stiffer at lower than 10 degrees heel, meaning that the roll motion induced by waves is smaller than in the case of a vessel marginally complying with regulations from the International Convention on Load Lines (ICLL, 1966). However, the formula for calculating the *s*-factor as per SOLAS 2020 assigns a very large value to the conditions marginally meeting the ICLL criteria; Namely: *s* = 0.955443.

Further calculations revealed that by increasing the required GZ value by just 1 cm, the result on the roll angle of a vessel in waves would be significant (around 4 %). Hence, it seems that it may be rational to investigate whether such an increase of the required maximum value of the righting arm is feasible from a practical implementation point of view and application to rules or guidelines.

References

1. Bole, M. & Lee, B.-S. (2006) Integrating Parametric Hull Generation into Early Stage Design. *Ship Technology Research* 53(3), pp. 115–137, doi: 10.1179/str.2006.53.3.003.
2. Bowditch, N. (1995) *The American Practical Navigator*. Scholarly Press.
3. Cummins, W.E. (1962) *The Impulse Response Function and Ship Motions*. Hydromechanics Laboratory Research and Development Report. Report 1661, available from: https://dome.mit.edu/bitstream/handle/1721.3/49049/DTMB_1962_1661.pdf [Accessed: May 02, 2021].
4. Das, S.K., Sahoo, P.K. & Das, S.N. (2006) Determination of Roll Motion for a Floating Body in Regular Waves. *Proceedings of the Institution of Mechanical Engineers, Part M, Journal of Engineering for the Maritime Environment* 220(1), pp. 41–48, doi: 10.1243/14750902M01904.
5. Faltinsen, O. (1990) *Sea Loads on Ships and Offshore Structures*. United States.
6. Fan, S. & Xia, J. (2002) *Simulation of Ship Motions – Coupled Heave, Pitch and Roll*. Perth, Australia: Centre for Marine Science & Technology. Technical Report No. 2002-35, CMST Project No. 366.
7. Fujiwara, T., Tsukada, Y., Kitamara, F., Sawada, H. & Ohmatsu, S. (2009) *Experimental Investigation and Estimation on Wind Forces for a Container Ship*. Proceedings of the Nineteenth International Offshore and Polar Engineering Conferences, Osaka, Japan, June 21–26, 2009.
8. Gourlay, T. & Lilienthal, T. (2002) *Dynamic stability of ships in waves*. In: Prandolini, L. (ed.) *Proceedings of Pacific 2002 International Maritime Conference*, Barton, A.C.T.: Institution of Engineers, Australia, pp. 434–441.
9. Hardin, E. (2013) *Simulating Wind Over Terrain: How to Build an OpenFOAM Case from GRASS GIS Digital Elevation Models*. North Carolina State University, Available from: https://1library.net/document/zp6ljg4q-simulating-terrain-build-openfoam-grass-digital-elevation-models.html [Accessed: May 02, 2021].
10. Hem Lata, W. & Thiagarajan, K.P. (2007) *Comparison of added mass coefficients for floating tanker evaluated by conformal mapping and boundary element methods*. 16th Australian Fluid Mechanics Conference, Gold Coast, Australia, 2–7 December 2007.
11. ICLL (1966) International Convention on Load Lines – 66/88 as revised in 2003.
12. ITTC (2011) *Numerical Estimation of Roll Damping*. ITTC Recommended Procedures and Guidelines 7.5-02-07-04.5.
13. Journée, J.M.J. (2001) *Theoretical Manual of SEAWAY*. Report 1216a. Delft University of Technology.
14. Journée, J.M.J. & Massie, W.W. (2001) *Offshore Hydromechanics. 1st Edition. Chapters 6, 7, 8*. Delft University of Technology.
15. Kawahara, Y., Maekawa, K. & Ikeda, Y. (2012) A Simple Prediction Formula of Roll Damping of Conventional Cargo Ships on the Basis of Ikeda's Method and its Limitation. *Fluid Mechanics and its Applications* 2(4), doi: 10.1007/978-94-007-1482-3_26.
16. Larsen, M.M. (2013) *Time Domain Simulation of Floating, Dynamic Marine Structures Using USFOS*. MSc Thesis. Trondheim, Norway: Norwegian University of Science and Technology.

17. MILLER, E.R., SLAGER, J.J. & WEBSTER, W.C. (1974) *Development of a Technical Practice for Roll Stabilization System Selection*. NAVSEC Report 6136-74-280.

18. SALEHI, M., GHADIMI, P. & ROSTAMI, A.B. (2014) A more robust multiparameter conformal mapping method for geometry generation of any arbitrary ship section. *Journal of Engineering Mathematics* 89, pp. 113–136, doi: 10.1007/s10665-014-9711-8.

19. SALVESEN, N., TUCK, E.O. & FALTINSEN, O. (1970) *Ship Motions and Sea Loads*. Society of Naval Architects and Marine Engineers.

20. SCHMITKE, R.T. (1978) *Ship Sway, Roll and Yaw Motions in Oblique Seas*. Society of Naval Architects and Marine Engineers.

21. SOLAS (2020) Save Our Lives at Sea.

22. SZULCZEWSKI, P. (2017) *A Method of Identification of a Set of Parameters of Decisive Impact on Safety of Cargo Ships in Damaged Conditions*. PhD Thesis. Gdańsk: Gdańsk University of Technology.

23. TRAINTAFYLLOU, M.S., BODSON, M. & ATHANS, M. (1983) Real time estimation of ship motions using Kalman filtering techniques. *IEEE Journal of Oceanic Engineering* 8, 1, pp. 9–20, doi: 10.1109/JOE.1983.1145542.

24. TUNALEY, J.K.E. (2013) *An Examination of the Taylor Standard Series of Hull Forms*. Available from: https://campus.fi.uba.ar/pluginfile.php/266853/mod_page/content/22/Taylor-Standard-Series.pdf [Accessed: May 02, 2021].

25. WANG, K., ZHANG, X., ZHANG, Z.-Q. & XU, W. (2012) Numerical analysis of added mass and damping of floating production, storage and offloading system. *Acta Mechanica Sinica* 28, pp. 870–876, doi: 10.1007/s10409-012-0075-x.